Int. J. of Geology & Earth Sci., 2018

International Journal of Geology and Earth Sciences

ISSN 2395-647X www.ijges.com
Vol. 4, No. 4, December 2018
doi:10.32937/IJGES.4.4.2018.14-34

Research Paper

Geomorphological Classification of Volcanic Cones in the Itasy Volcanic Field, Central Madagascar

Tsilavo Raharimahefa[1*] and Christine Rasoazanamparany[2]

Corresponding Author:* ***Tsilavo Raharimahefa* ✉ *Tsilavo.Raharimahefa@uregina.ca*

Received on: 29th July, 2018 Accepted on: 30th August, 2018

The Itasy Volcanic Field (IVF) is a monogenetic volcanic field located in the central highlands of Madagascar and is characterized by numerous volcanic cones displaying various geomorphological landforms. The IVF was a result of Pliocene to Quaternary volcanic eruptions and mainly composed of basaltic volcanic cones and trachyte domes. This paper aims to describe and to establish a geomorphological classification of basaltic volcanic cones within the IVF, based on their morphometric characteristics such as shape and diameter of the cone base; slope of the flanks of the edifice, and height of the crater relative to the cone base. Digital Elevation Model (DEM) data from Advanced Spaceborne Thermal Emission and Reflection Radiometer (ASTER) and Shuttle Radar Topography Mission (STRM) were used, coupled with remote sensing data from Google Earth Pro and field investigation. DEM and imagery analyses and processing were performed using ArcGIS and Global Mapper. Five types of major basaltic volcanic landforms were identified within the IVF: semi-circular cones (e.g. Kasigie cone), representing 8.39% of the identified cones; symmetric and asymmetric horseshoes-shaped edifices (e.g. Mananasy and Fasia cones), which are the most dominant 74.8% of the cones; fissure cones (e.g. Mandetika cone) forming 5.34% of the cones; multiple clustered ε-shaped breached cones forming 6.1% of the volcanic cones (e.g. Ambohitritainerina cone) and single cone with multiple craters (e.g. Ambohitromby cone), which represent 6.1% of the cone. This contribution enables the characterization of morphological types of the volcanic cones within the IVF.

Keywords: Itasy Volcanic Field, Digital Elevation Model, Cone morphology, Volcanic morphometry

Introduction

Monogenetic volcanic cones represent a common expression of continental volcanism (Németh, 2010) and occur in a variety of tectonic settings most commonly extensional and/or intracontinental rifting (Chorowicz, 2005; Petit and

[1] Department of Geology, 3737 Wascana Parkway, University of Regina, Regina, Saskatchewan, Canada.
[2] Department of Geology and Environmental Earth Science, 118 Shideler Hall, 250 S. Patterson Ave., Miami University, Oxford, Ohio, United States of America.

Déverchère, 2006; Putirka and Platt, 2012) and subduction settings (e.g., Hasenaka and Carmichael, 1985). The term monogenetic eruption has a wide range of definitions, but early definitions refer to small-volume eruptions (≤1 km^3) which are produced by a single episode of volcanic activity without subsequent eruptions (Rittmann, 1963; Connor and Conway, 2000). Depending on their eruptive styles, monogenetic vents can occur as scoria cones, tuff cones or maars (Connor and Conway, 2000; Martin and Németh, 2006; Valentine *et al*., 2006; Valentine and Perry, 2007; Valentine and Gregg, 2008). They often exhibit a wide range of eruptive styles from relatively non-explosive (e.g., effusion of lava flows) to highly explosive (e.g., violent strombolian), however, the associated volcanic hazards are generally localized compared to those of large silicic stratovolcanoes. Nonetheless, because the location of volcanic activity within a given volcanic field tends to shift over time, they could pose potential threat to important infrastructure (Connor *et al*., 2009). Numerous studies have focused on the morphology of monogenetic volcanoes and their morphometric parameters, with the aim of (1) reconstructing magma-feeding dikes in monogenetic system (e.g., Corrazato and Tibaldi, 2006); (2) obtaining insight into growth and degradation of cinder cones (e.g. Valentine *et al*., 2007); (3) providing basic information about the relative age of volcanic eruptions (e.g., Wood, 1980a,b; Hasenaka and Carmichael, 1985); or (4) establishing morphological classifications of volcanic cones (e.g. Wood, 1980a; Doniz-Paez, 2015). In addition, the morphological features or the shape of volcanic cones have also been used in several studies to decipher their tectonic or structural settings and their emplacement modes (Riedel *et al*., 2003; Rodríguez *et al*., 2010; Bemis *et al*., 2011; Inbar *et al*., 2011; Kereszturi and Németh, 2012; Di Traglia *et al*., 2014, Takada, 1994; Tibaldi, 1995; Corazzato and Tibaldi, 2006; Valentine *et al*., 2007; Dohrenwend *et al*., 1986). As such, geomorphological studies of volcanic cones are an essential step toward the understanding of how basaltic cinder cones form and evolved through time.

Over the last decade, Digital Elevation Models (DEM) from Advanced Spaceborne Thermal Emission and Reflection Radiometer (ASTER) and Shuttle Radar Topography Mission (STRM) have been extensively used in volcano geomorphology (Inbar *et al*., 2011, Grosse *et al*., 2012, Gong *et al*., 2016; Camiz *et al*., 2017); as they can provide important geomorphological parameters such as shape, slope, gradients, altitudes and relief (Kervyn *et al*., 2008). Several previous works have highlighted the importance and the full potential offered by DEMs in many aspects of volcanological studies (Fornaciai *et al*., 2012; Kervyn *et al*., 2012; Gong *et al*, 2016; Favalli and Fornaciai, 2017; Lenhardt *et al*., 2018) including the study of genesis and evolution of volcanic edifices (Wood, 1980a,b; Thouret, 1999, Prima and Yoshida, 2010), and the relationship between topography and hazards related to volcanic landforms (e.g. Hickson *et al*., 2013). This study focuses on the Itasy Volcanic Field (IVF), which is one of the Quaternary volcanic fields in central highland of Madagascar. The field is composed of hundreds of volcanic cones of different sizes, shapes, slopes and reliefs. However, little or no effort has been dedicated for the characterization of the morphology and morphometric analyses of these cones. In addition, mafic volcanic fields in the central highland of Madagascar were believed to be related to the extension of the diffuse southern

arm of the East African rift system (Kusky *et al*., 2010); therefore the IVF represents an ideal location to study the morphology of volcanoes associated with this diffuse plate boundary. The main objectives of this paper are therefore to: 1) define and classify the different geomorphological type of volcanic cones within the IVF excluding the domes and maars, and 2) perform morphometric analysis of selected and representative volcanoes types within the field. The geomorphological classification of the IVF basaltic volcanic cones are derived from field investigation, analyses of DEMs and high-resolution satellite images and aerial photos from Google Earth and Global Mapper online data sources. Five different types of basaltic volcanic cones were identified, and each type was defined on the basis of its shape, size, topography and morphometry; those reflect the magma budget, chronology of eruption and insight to their emplacement. This work contributes to a better understanding of volcanic landforms in the IVF and monogenetic volcanic fields in general.

Geological Setting

The Itasy volcanic field represents one of the Quaternary mafic volcanic fields in the central highland of Madagascar and covers an area of approximately 1600 km^2 (Figure 1). The volcanic

Figure 1: Geologic Map of the Itasy Area (Modified From Razafinimparany et al., 1974) and Location of Volcanic Cones

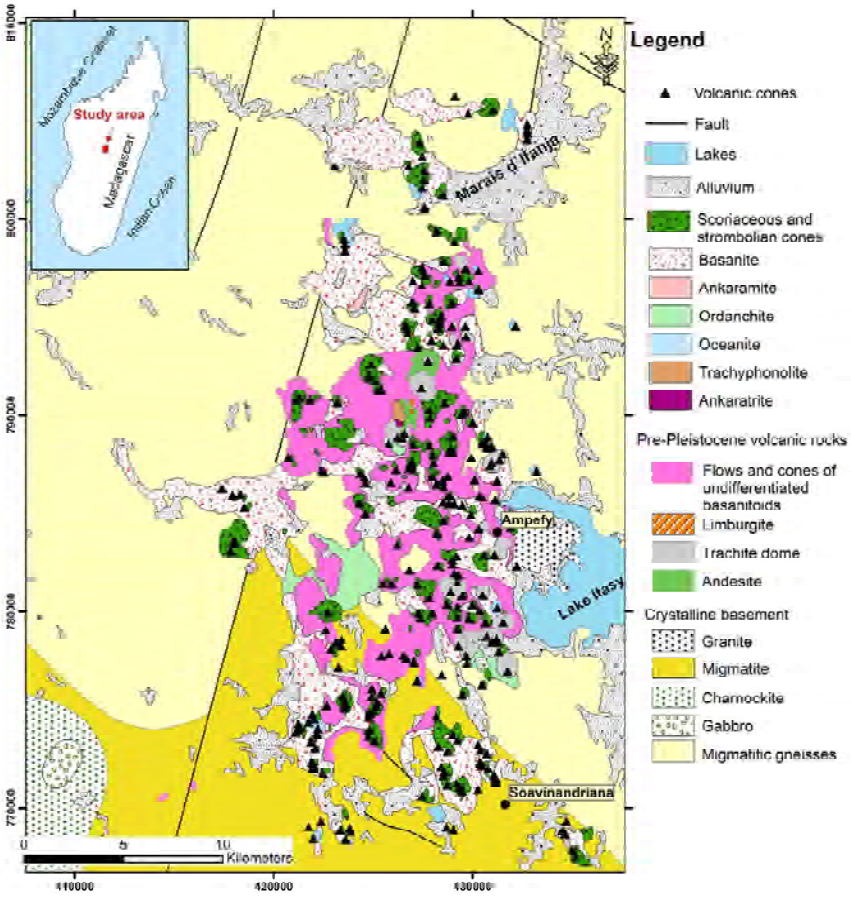

field was emplaced on a crystalline basement consisting mainly of deformed gneisses, and migmatites (Razafinimparany *et al*., 1974) and are Precambrian in age (Tucker *et al*. 2014). The volcanic field forms a north-south trending belt of scoriaceous and strombolian volcanic cones that are delimited to the west by a major north-trending fault, to the east by the Itasy Lake, to the north by the Ifanja marsh (Marais d'Ifanja), and to the south by the village of Amparaky (Figure 1).

The volcanic field contains a wide range of volcanic landforms including scoria cones, maar craters, trachytic domes and lava flows. The cause and origin of the basaltic volcanism in central Madagascar remain controversial, but recent studies have invoked partial melting of metasomatized sub-continental lithospheric mantle in response to lithospheric thinning and extension (e.g. Melluso *et al*., 2011, 2016). In addition, radiometric age determinations are still lacking for the Itasy volcanic rocks, but some studies indicated that the volcanic field has been active since the Pliocene (Bussier, 1957; Melluso *et al*., 2018). Peat associated with a phreatomagmatic maar deposit near Lake Itasy yielded a radiocarbon age of 8505±90 years BP (Vogel, 1970), suggesting that the volcanic activity has continued to as recently as Holocene and that the field remains volcanically active. Bussiere (1975) provided the relative chronology of volcanic activity in the IVF, and suggested that the very early phase of activity was dominated by surface eruptions and intrusions of lava domes and lava flows of Kasigie with trachytic and trachy-phonolite compositions. This was followed by the eruptions of the oldest flows of alkali basalt and olivine nephelinite (ankaratrite), then by the eruption and intrusion of trachytic dome and trachy-phonolite lavas of Andranonatoa. These phases were followed by the eruption of basanite, trachy-andesite and tephrite flows. The final phase of volcanic activity was represented by maars eruptions (Bussiere, 1957).

The Itasy area is also known as one of the most seismically active regions of Madagascar (Rindraharisaona *et al*., 2013; Bertile and Regnoult, 1998), and is associated with hot springs activity, further indicating that the IVF is essentially an active field. Bouguer gravity anomalies and seismic data indicated that a low-velocity zone occurs beneath this area (Rechenmann, 1981; Bertil and Regoult, 1998) which is believed to be related to a shallow upwelling of asthenosphere (65 km depth; Rakotondraopianina *et al*., 1999; Rakotondraopianina, 1992). This upwelling of asthenosphere has been proposed to cause the uplift of the Itasy-Ankaratra regions over the past 10-15 Ma (Bertil and Regoult, 1998), as well as the high concentration of seismic activity and mafic volcanism in this part of the highlands. Furthermore, Kusky *et al*. (2010) suggested that the mantle upwelling is induced by an active rifting or could be the result of a plume-rift interaction. This active rifting is interpreted to be associated with the southward extension of the Somalian-African diffuse plate boundaries, one segment of which runs along the northern and central parts of Madagascar and has triggered the present day neotectonic movement in these regions (Kusky *et al*., 2010).

Methodology

Geomorphological classification of basaltic volcanic cones in this study uses different approaches including field investigation, analyses of DEMs, high-resolution satellite images and aerial photos from Google Earth and Global Mapper online data sources. Because of the lack

of up-to-date topographic maps in most parts of Madagascar, DEMs and satellite images were used primarily to produce details maps of the volcanic cones in the IVF. In addition, morphological parameters (Wood, 1980a,b; Doniz-Paez, 2015) such as cone base maximum (W_{co_mx}) and minimum (W_{co_mi}) diameters, area (A) covered by the edifice boundary, volume (V) enclosed between the DEM surface of the cone and the 3D basal surface of the edifice, crater maximum (W_{cr_mx}) and minimum (W_{cr_mi}) diameters, and cone height (H_{co}), as well as slope (S) of the cone's flanks have been measured in order to effectively define the shape of a given volcanic cone, height-cone basal diameter ratio (H_{co}/W_{co}) where the cone basal diameter (W_{co}) is derived from the average of maximum and minimum axes of the basal best fit ellipse i.e. $Wco=(W_{co\_mx}+W_{co\_mi})/2$. The degree of ellipticities (R_f) of both cone base and crater rim for the single crater selected cones have also been calculated, where Rf is defined by the ratio of long axis to short axis of the cone base or crater rim.

Aerial and Satellite Images

Remote sensing data are very useful in mapping lava flows, faults, and various geological features. Basaltic cones were initially located and identified using aerial and satellite images, which were extracted from Google Earth and Global Mapper digital online data. Only well-preserved cones were mapped and counted. Images acquired during dry seasons (May to September) were chosen because during those times the volcanic cones have less vegetation and most of the images are cloud-free, thus increase the ability to map the boundary of lava flows, and enhanced the detection of cone bases and crater cones. All images were georeferenced and projected into Laborde coordinate system (a metric projection system), the official coordinate system used in Madagascar. All 2D images were from Global Mapper and 3D images were extracted from Google Earth Pro, which provided a better spatial resolution.

Field Study

Fieldwork was crucial because lava flows often merge with the surrounding rocks, leading to a difficult determination of boundary limits of lava flows and the base of the volcanic edifices on satellite images. The Itasy volcanic field (IVF) and surrounding areas were visited during the summers of two consecutive years, 2016 and 2017. In general, most volcanic cones are well-preserved and provided good outcrop exposures; however, some of the older cones are party buried by flows and tephra associated with younger cones. Selected cones with various altitudes were studied in details. Handheld GPSs were used to locate each volcanic cone and to record the elevations. The Garmin GPS provided a horizontal accuracy of 3 m (horizontal datum WGS84) and a vertical accuracy of 15m, which was manually calibrated to a known elevation to get an elevation accuracy of 3m. In addition, ground control points (GCP) were selected and corrected to geoid heights (vertical datum Earth Gravitational model 1996 known as EGM96), and the GCP data were used to check the accuracy of the ASTER and SRTM Digital Elevation Models (DEMs). The heights of the cones and slope of the flanks were measured in the field using GPS and Brunton Compass respectively, and were used to assess the heights extracted from DEMs.

Digital Elevation Model (DEM)

Both ASTER GDEM 1 arc-second and SRTM 1-arc-second DEMs were used in this study. The DEMs were accessed and downloaded using

Global Mapper online data and treated in both ArcGIS 10.5 and Global Mapper software. DEMs data were also reprojected into Madagascar Laborde coordinate system. The ASTER GDEM 1 arc-second elevation model was generated from stereo-pair satellite images gathered by ASTER satellite, which is a passive system and provide a spatial resolution of 30 meters with a vertical accuracy of 20 m (Grosse *et al*. 2012). The SRTM 1-arc-second global elevation is derived from an active system (radar data) and offers a void filled data for the study area at a horizontal accuracy of 30m and a vertical accuracy as low as 5m (Rodriguez *et al*., 2006). Because this study focuses more on regional classification of IVF's monogenetic cinder cones, the spatial resolution of 30 meters is sufficient to obtain valuable data. The ASTER DEM was used mainly for a regional context and overall assessment of the variation in elevation in the IVF (Figure 2), whereas detailed analyses such as slopes, heights and contours of selected

Figure 2: Digital Elevation Model Derived From Aster Data With Location of the Volcanoes Studied, The Dem Map Shows The Variation Of Elevation In And Around The Volcanic Field

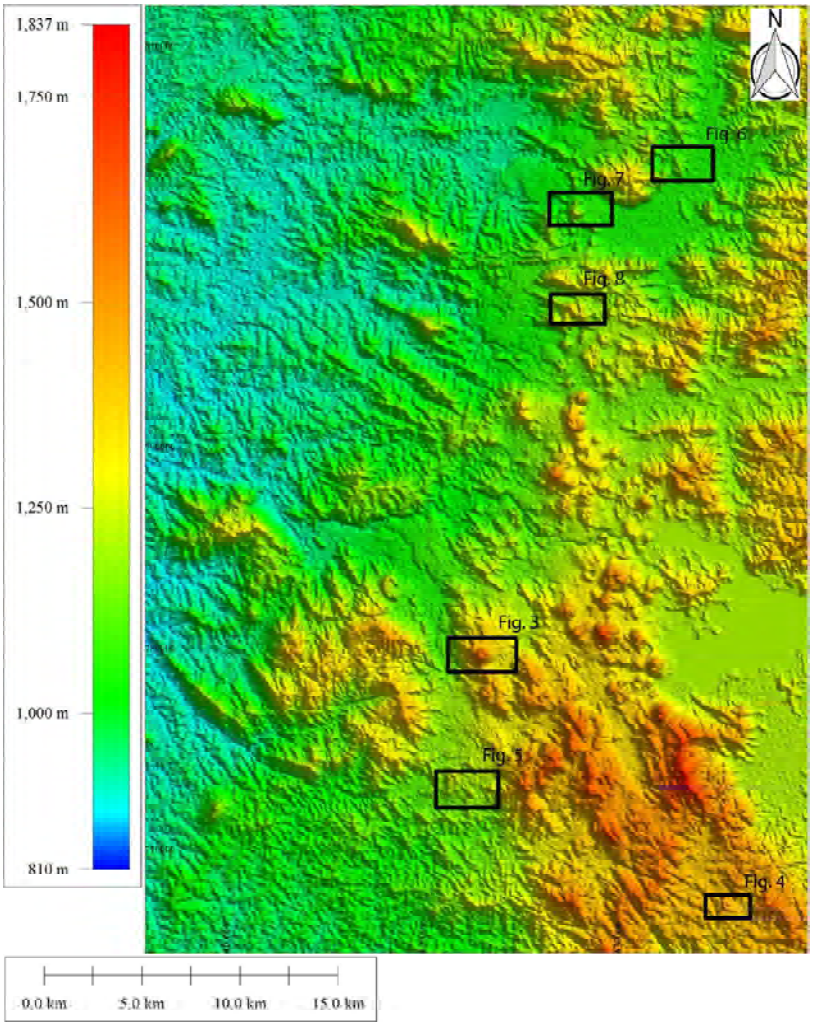

cones were derived from SRTM DEMs (Figure 3 to 8). Contour lines were extracted and draped on top of the elevation map; then topographic cross-sections were built. Slope maps were also developed to evaluate the variation of slope on the flanks of the volcanoes. The base of each monogenetic cones or edifice was defined by the lowest contour line around the cone and the cone basal plane elevation was estimated from average pixels values of the DEM in the basal ellipse shape outline. Furthermore, field identification and google earth were used to correct the edifice boundaries. From the DEMs, we calculated the average slope (S), the area (A), the volume (V), the cone basal diameters (W_{co}), cone height (H_{co}), and approximate crater diameters (W_{cr}).

Geomorphological Classification of IVF Volcanoes

The results of the morphometric analysis of the selected cones are given in Table 1. ASTER DEM data shows that elevation in the IVF ranges from ~800m to ~1,900m above sea level (a.s.l). As

Figure 3: Semi-circular Cone of Kasigie

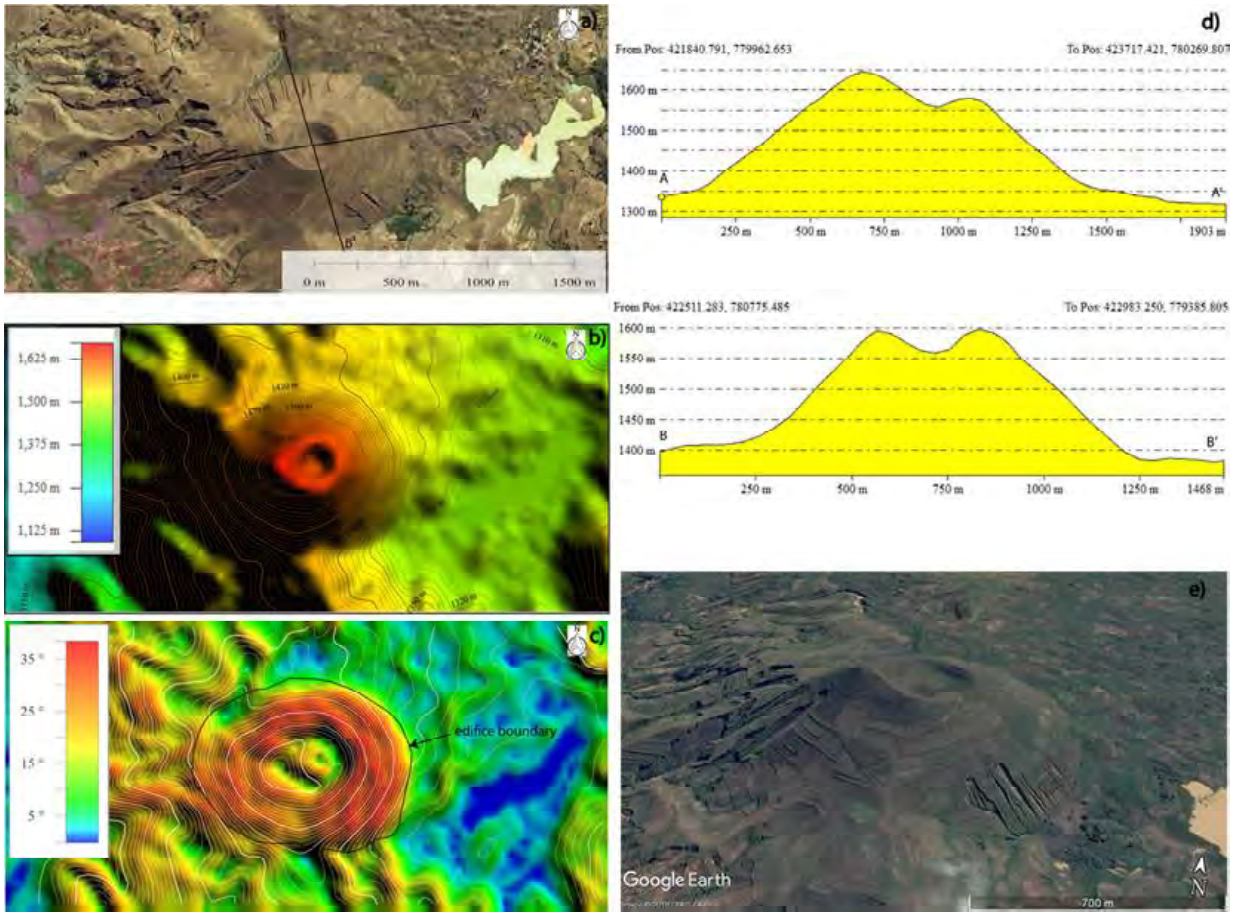

Note: a- satellite image showing the plane view of Kasigie; b-DEM showing the change of elevation around the Kasigie cone; c- slope map of Kasigie; d- topographic profiles of transect AA' and BB' seeing on fig. 3-a; e- Google Earth 3D view of Kasigie.

illustrated in Figure 2, there is an increase of elevation from west to east within the volcanic field. We have identified 131 mafic volcanic cones within the study area (Figure 1) which did not include maar eruptive centers and trachytic domes. The morphometric parameters (e.g. H_{co}, W_{co}, S) and their shapes have allowed us to classify the volcanic cones into five morphological types (Figure 3 to Figure 8).

Semi-Circular Cones

These cinder cones exhibit circular to semi-circular shapes with closed craters. They are characterized by one single cone with a single crater. In general, the crater rims display a wide range of size, small craters exhibit an aspect ratio (W_{cr}/W_{co}) of crater rim diameter/cone base diameter of < ¼, whereas, large craters display W_{cr}/W_{co} ratios of > ½. Semi-circular cones are quite common in the IVF and they represent 8.39% of the identified cones.

One of the best representative cones of this semi-circular type is the well-preserved volcanic cone of Kasigie, also known as Kasigie Mountain. It is located in the central southwestern part of

Figure 4: Horseshoe-shaped Asymmetric Fasia Volcanic Cone

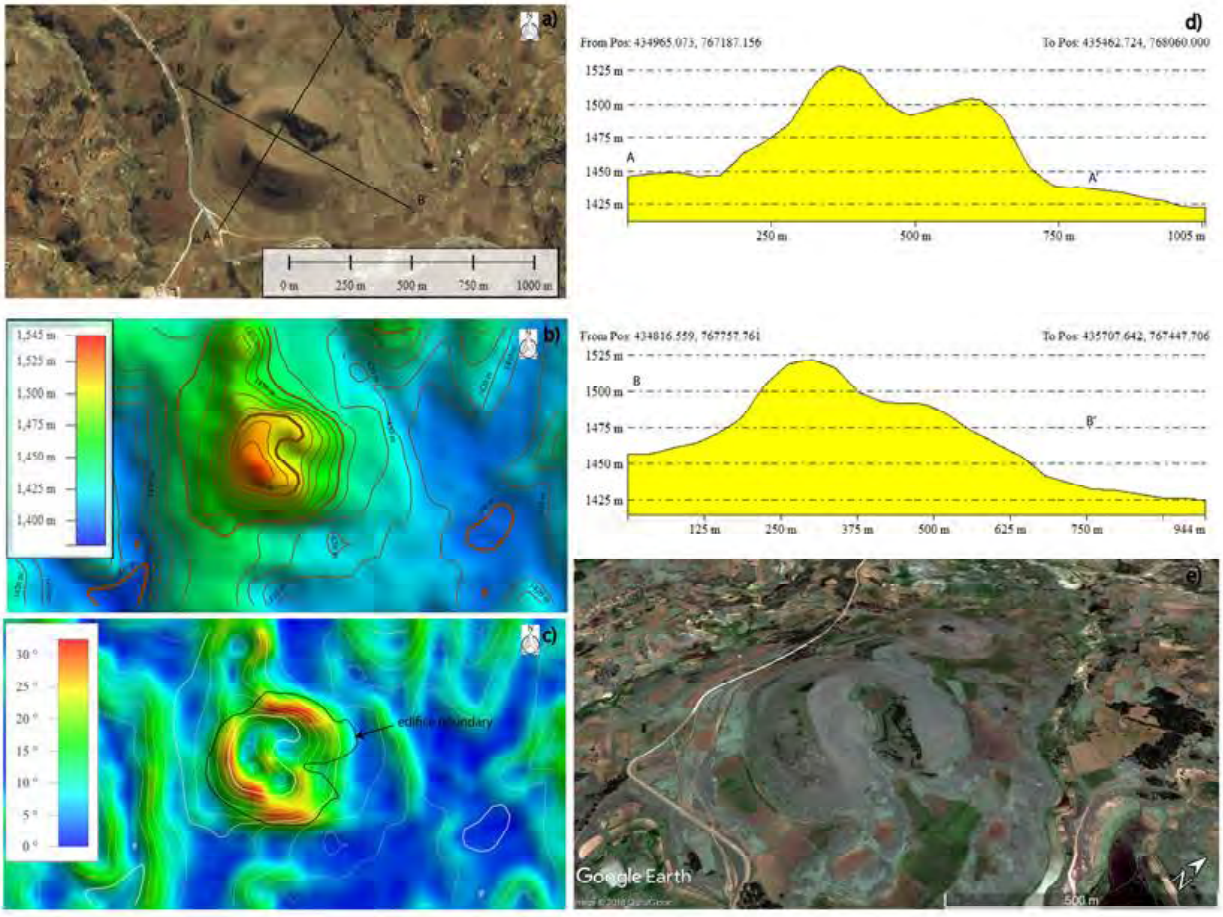

Note: a- satellite image showing the plan view of Fasia cone; b-DEM of Fasia cone; c- slope map of Fasia cone; d- topographic profiles of transects seeing on fig. 4-a; e- Google Earth 3D view of Fasia cone.

Figure 5: Horseshoe-shaped Mananasy Symmetric Volcanic Cones

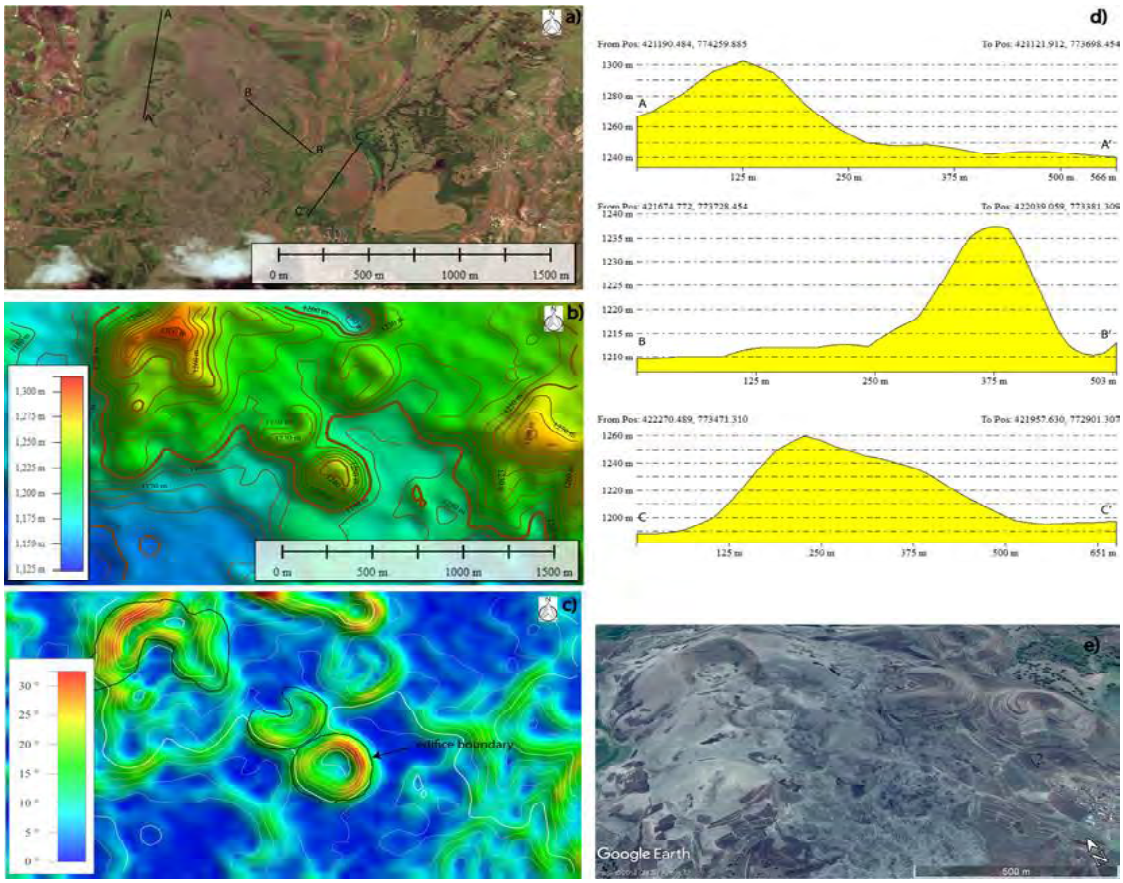

Note: a- satellite image showing the plan view; b-DEM showing the change of elevation around the Mananasy cones; c- slope map showing the variation of slope angles; d- topographic profiles of transects seeing on fig. 5-a; e- Google Earth 3D view of the cones.

the volcanic field and is surrounded by massive lava flows. Kasigie volcanic cone is mainly composed of unconsolidated tephra, volcanic bombs and is associated with extensive lava flows extending up to 5 km from the cone. The volcanic edifice is tall, isolated with a small, single tear-drop shaped crater (Figure 3a, b, d) seating on an area of 0.99km^2 (Table 1). Kasigie itself reaches an elevation of ~ 1,650 m above sea level (a.s.l) and a cone maximum height of ~250 m (H_{co}) with steep slope average of 40° (Figure 2c). It has a cone base maximum diameter of 1,260m (W_{co_max}), a cone base minimum diameter of 1,000 m, crater maximum diameter of 330m and a minimum diameter of 250m. The flanks of the Kasigie Mountain are heavily eroded by long, thin and deep gullies (lavaka) that are concentric and pointing toward the center of the crater. The DEM-based volume of the cone from the 3D edifice yields a volume of 0.0731km^3.

Horseshoe-Shaped Cones

This type of cinder cone exhibits horseshoe-like shape and is typically breached. It represents the most dominant (by number) morphological type in the IVF and comprises 74.8% of the total

Figure 6: Fissured Cone Known as Mandetika Cone

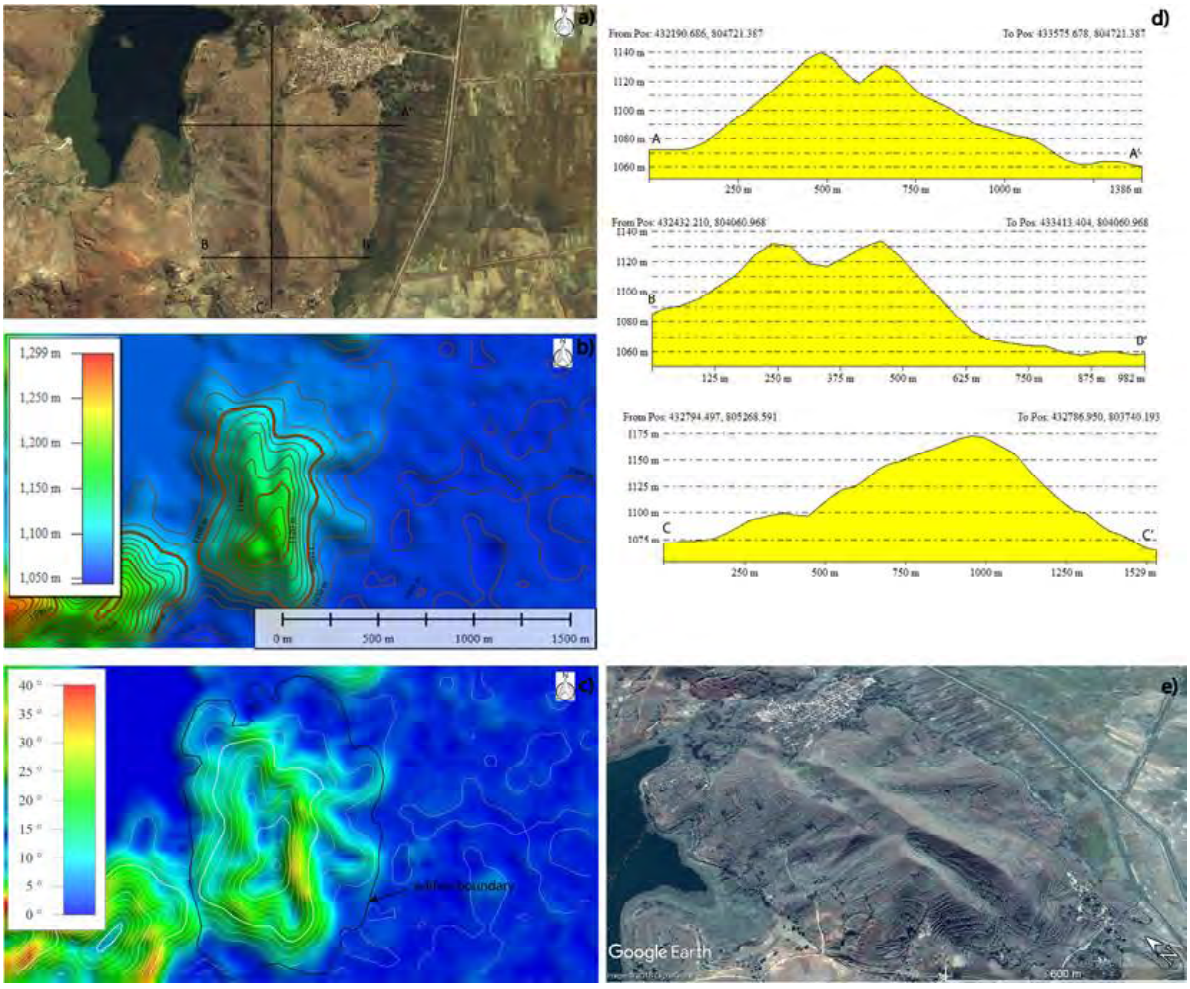

Note: a- satellite image showing the plan view of the cone; b-DEM showing the change of elevation around the fissure cone; c- slope map showing the variation of slope angles; d- topographic profiles of transects seeing on fig. 6-a; e- Google Earth 3D view of the cones.

volcanic cones. They are generally small and tend to have circular cone base with W_{co} (i.e. diameters of cone bases) usually less than 750m and an average height of 100 meters. This morphological type can be further subdivided into two subgroups: asymmetric and symmetric horseshoe-shaped cones.

Asymmetric Horseshoe-Shaped Cones

This subgroup is characterized by a horseshoe-shaped breached cone with one side being slightly longer than the other. The best example of asymmetric horseshoe breached cones is the Fasia cone. This cone is located in the southeastern tip of the volcanic field, on the eastern side of the main road to Faratsiho, approximately 5km from the town of Soavinandriana. It is characterized by a cone base diameter of ~510m, a crater rim diameter of ~210m, a maximum pick of 1,530m a.s.l and a maximum height of 100m above the surrounding

Table 1: Morphometric Parameters for the Representative Volcanic Cones in the IVF

Name of the Cone	Elevation a.s.l (in m)	H_{co} in m	W_{co_mx} in m	W_{co_mx} in m	W_{co}	H_{co}/W_{co}	W_{cr_mx} in m	W_{cr_mi} in m	W_{cr}	S (in °)	Rf_{co}	Rf_{cr}	V (in m^3)	Area in Km^2
Kasigie	1650	250	1260	1000	1130	0.22	330	250	290	40	1.26	1.32	73157808	0.99
Fasia	1530	100	510	510	510	0.20	210	210	210	30-35	1	1	4410157	0.2227
Mananasy (NW cone)	1305	65	730	730	730	0.09	320	320	320	15-32	1	1	5069774	0.3099
Mananasy (middle Cone)	1238	28	400	400	400	0.07	220	214	217	20	1	1.02	1240878	0.1086
Mananasy (Southern Cone)	1260	78	420	420	420	0.19	170	170	170	20-30	1	1	3385192	0.1556
Mandetika	1150	100	1500	950	1225	0.08	-	-	-	32	1.57	-	33358726	1.312
Ambohi-tritainerina	1270	200	1138	860	999	0.20	-	-	-	25-38	1.32	-	37100476	0.753
Ambohi-tromby	1390	165	800	600	700	0.24	-	-	-	15-35	1	-	36658705	1

Note: H_{co} is the cone height, W_{co_mx} is the cone basal maximum diameter, W_{co_mi} is the cone basal minimum diameter, W_{cr_mx} is the crater width maximum diameter, W_{cr_mi} is the crater width minimum diameter, S is the slope of the flanks, Rf is the degree of ellipticity for cone base or crater, V is the DEM-based volume of the cone from the 3D edifice, and A is the surface area covered by the edifice.

valley (Figure 4a, b, d). The slope of the flanks varies, with outer flanks average slope of 30° and inner flanks of 35° (Figure 4d). The cone covers an area of 0.222km^2 and has a DEM-based volume of 0.0044km^3 (Table 1). It is composed mainly of pyroclastic fragments with the breached rim at the SE side of the cone. In addition, it is associated with two smaller satellite cones, which are located on the northern side of the cone.

Symmetric Horseshoe Cones

This subgroup is also characterized by a horseshoe-shaped breached cone; however, the two sides have similar size and shape. Examples of symmetric horseshoes-like cones are the three basaltic cones located near the town of Mananasy in the southern part of the volcanic field. The cones are small, closely spaced (less than 5m distance) and with cone bases diameters generally less than 700m, and with moderate to steep slope (Figure 5d and 5c). The slopes of the outer flanks are usually shallower than the inner flanks (Figure 5d). The lava flows associated with these volcanoes extend up to 2 km from the source cone(s), and composed of massive basaltic lava. The morphometry of these three selected cones are as follow: 1) northwestern cone (Figure 5a, 5c A-A'): 1,305m a.s.l. with a maximum height of 65m above the surrounding valley, cone base diameter of ~730m, crater rim diameter ~320m, slopes ranging from 15° to 32°, covers an area of 0.309km^2, and a volume of 0.0050km^3. 2) Middle cone (Figure 5a, 5c B-B'): stands 1, 238m a.s.l with only 28m

height, cone base diameter of ~400m, crater rim diameter ~220m, average slope of 20°, seats on an area of 0.108 km^2 and a cone volume of 0.0012km^3. 3) Southern cone (Figure 5a, 5c C-C'): , stands 1,260 a.s.l with 78m height relative to the valley, covers an area of 0.155km^2, cone base diameter of ~420m, crater rim diameter ~170m, slopes ranging from 20° to 30°, and a DEM-based volume of cone from 3D edifice of 0.0033km^3.

Fissure Cones

This type is represented by two parallel ridges separated by an elongated depression or fissure (Figure 6a,e). The fissure type makes 5.34% of the identified cones in the IVF. The best example of this type is the Mandetika fissure cone (named after the nearby lake) and is located in the northern tip of the volcanic field, in between Lake Mandetika and Marais d'Ifanja. The cone appears to be made of several eruptive vents that are aligned along a fissure (Figure 6 a,b,d). It forms an elongated and flat laying cone with a maximum pick of 1,150 m a.s.l. and stands 100 m above the surrounding valley. The cone base maximum elongation is 1,500m and a minimum diameter of 950m. It stands on an area of 1.312km^2 and yields a DEM-based cone volume of 0.0333km^3. The slopes display slight variation from 25 to 32°, with outer flanks showing a maximum slope of 32° (Figure 6c). Our field investigation reveals that the fissure of the Mandetika cone is located along a N-S striking fault zone.

Multiple Clustered Breached "ε" (Epsilon)-Shaped Cones

This morphological type is represented by coalescent breached cones where the openings of the cones seem to face slightly one another, though parts of the cones are still connected, forming ε-shaped crater rim (Figure 7a, b, c). Multiple ε-shaped breached cones accounted for 6.1% of the volcanic landform in the volcanic field. The best example of this type of cone is located near the town of Ambatolampy in the northern part of the volcanic field. The multiple cones are locally known as Ambohitritainerina. The individual crater is generally small (diameter < 300 m) and the flanks are moderate to steep dipping (25° to 38°) (Figure 7c). Altogether, the best fit ellipse of the cone base displays a long axis of 1,138 m and a short axis of 860 m. Although individual cone appears to be small, they are typically associated with extensive flows that can extend up to 4 km from the source cone(s). The maximum elevation of the Ambohitritainerina ε-shaped breached cone is 1,270 m a.s.l and the pick stands ~200m above the surrounding lava flows. The cone is built on 0.753 km^2 area and with a DEM based volume of 0.0371 km^3 (Table 1).

Multiple Craters in One Single Rim

This type of cone is represented by a single cone with multiple craters that often interfere with each other. As illustrated in Figure 8, these multiple craters appear to be surrounded by a single larger crater rim. In most cases, the craters are randomly distributed and scattered within the cone, however, they can also be aligned along the long axis of the cone base. This morphological type forms 3.8% of the identified cones within the volcanic field, and their crater rims may or may not be ruptured. The best example is located near the town of Tsarazaza (east of the town). The peak of the cone is 1,390 m a.s.l (locally known as Ambohitromby) and it stands 165m above

Figure 7: Multiple Clustered -shaped Cone

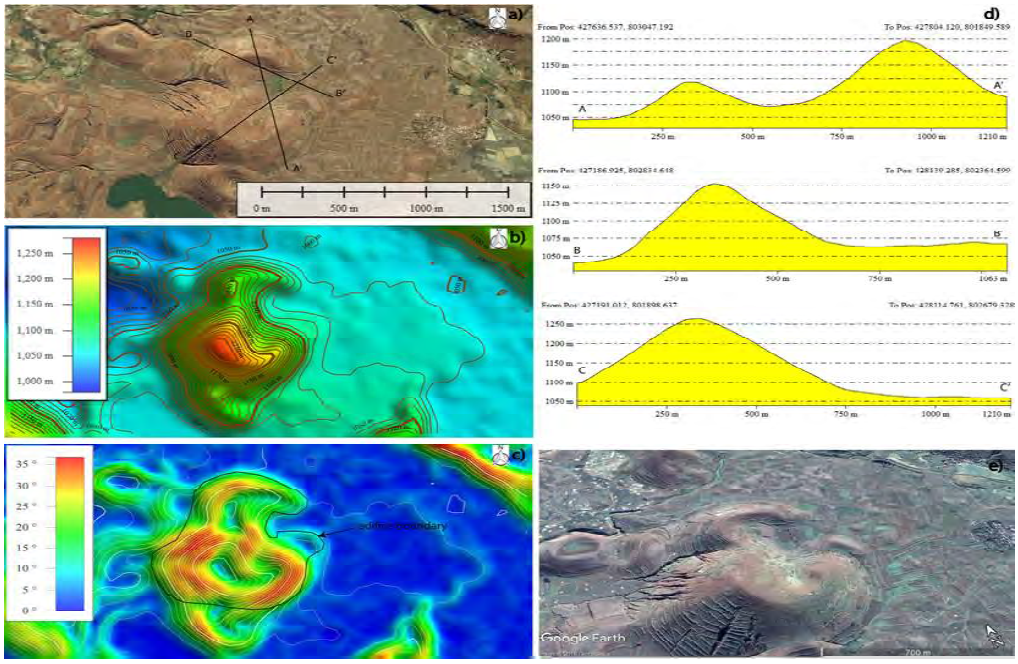

Note: a- satellite image showing the plan view of the Ambohitritainerina; b-DEM showing the change of elevation around the cone; c- slope map showing the variation of slope angles; d- profiles of transects seeing on fig. 7-a; e- Google Earth 3D view of the cones.

Figure 8: Cone with Multiple Crater Vents Grouped Within One Larger Rim

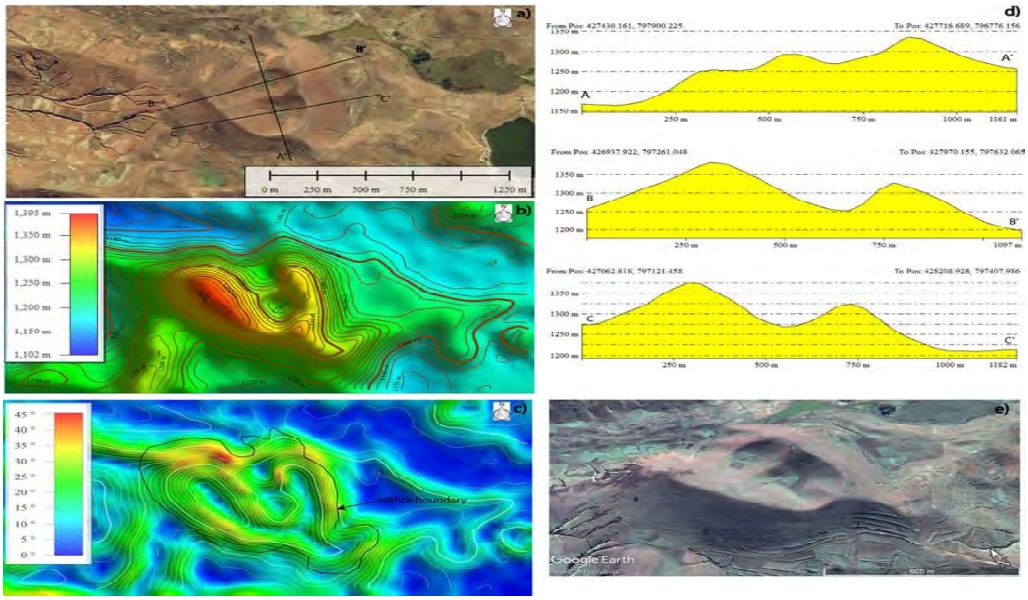

Note: a- satellite image showing the plan view of the cone; b-DEM showing the change of elevation; c- slope map showing the variation of slope angles; d- profiles of transects seeing on Figure 8-a; e- Google Earth 3D view of the cones.

ground with gentle to moderately dipping slopes (~15° to 35°) (Figure 8c and 8d). The composite cone base has a maximum diameter of 800m and minimum diameter of 600m. The cone covers an area of 1km^2 and yields a DEM-based cone volume of 0.0366km^3. It contains two craters, and each crater has approximately a diameter of 200 m.

Discussion

Volcanic cones in the IVF are well-preserved and can be classified using both qualitative and quantitative (Wood, 1980a, b) morphometry parameters measured from DEMs and field observations. Simple morphostructural study and classification of volcanic cones have been used in other volcanic fields (Dóniz-Páez, 2015; Gong *et al*., 2016) and can be considered as a starting point in studying the geomorphology of monogenetic basaltic cones (Dóniz-Páez, 2015).

Our remote sensing analysis and ArcGIS mapping reveal that the IVF contains more than 131 basaltic cinder cones that are distributed over an area of ~ 1600 km^2. These cinder cones can be classified into five major morphological types, including, semi-circular-shaped, horseshoe-shaped, multiple clusters -shaped, fissure and multiple craters volcanoes. Based on the current data, the horseshoe-shaped volcanoes represent the most abundant volcanic edifices within the volcanic field (~74 %) whereas the multiple craters in a single rim volcano comprise 3.5% of the total edifices, and constitute the least representative morphology of basaltic cinder cones in the IVF. In addition, the data indicates that the number of semi-circular-shaped volcanoes is relatively small (~8%) with respect to horseshoe-shaped edifices but higher than those of multiples clusters ε-shaped breached cones (~6%) and fissure eruption (~5%). Higher abundances of horseshoe-shaped relative to other volcanoes types are also observed in other young volcanic fields such as the Tenerife volcanic field (Doniz-Paez, 2008) and Calatrava volcanic field (Becerra-Ramirez, 2013). The selected volcanic cones in the present work have a wide range of eruptive volumes, ranging from 0.0012 to 0.0731 km^3, consistent with typical cones associated with monogenetic system ($\leq$ 1 km^3; Kereszturi and Nemeth, 2013). Some studies have highlighted the relative importance of the topography of the emplacement area in controlling the shape of volcanic cones (e.g., Doniz-Paez, 2015). For example, in the Tenerife volcanic field, Canary Island, Spain, simple cones such as circular or semi-circular-shaped volcanoes tend to occur at a lower altitude area and almost flat topography (<10°), whereas more complex volcanic edifices such as multiple coalescent volcanoes are mostly found at higher altitude regions (Doniz-Paez, 2015). In the Itasy Volcanic Field, no coherent correlations between topography and morphological category have been observed. In fact, both semi-circular-shaped and multiples volcanoes occur essentially in the same geographic location (< 500 m), and horseshoe-shaped vents are distributed all over the volcanic field. This strongly suggests that pre-eruptive topography might not influence the shape of the cinder cones within the Itasy volcanic field. Nonetheless, the present data suggest that the spatial distribution of volcanic vents within the field can be attributed to some extent to topographic controls, as volcanic vents are mostly emplaced at higher altitude areas. Although we do not have sufficient data to assess the origin and preservation of the morphological features identified, the shapes of the IVF volcanic cones

could be attributed to several factors as we discussed below.

The semi-circular type identified in this study is in essence very similar to the simple cone of Corazzato and Tibaldi (2006) and the ring-shaped cones of Doniz-Paez (2015). This simple morphological type has been linked to the geometry of the feeding conduit, the amount and ballistic trajectory of pyroclastic material ejected from the cone, as well as the development and growth of the cone around a single eruption point (e.g. Corrazato and Tibaldi, 2006; Dóniz-Páez *et al*., 2008, 2011, 2012; Kereszturi and Németh, 2012). Similarly, the horseshoe-type could also develop from a single eruption point, however, breaching or opening of the craters are often interpreted to be controlled by the slope of the pre-eruptive topography. Nonetheless, other factors such as wind direction during the eruption and the geometry and orientation of magma feeding dikes have also been proposed to explained this morphological feature (Doniz-Paez, 2015; Tibaldi and Lagmay, 2006; Kereszturi and Németh, 2012, 2013a,b). The fissure-type cones are generally interpreted to form as the result of eruptive episode from a multiple eruption points along a fissure. The Mandetika cone lies within the path of a major basement fault, suggesting that it may have erupted along pre-existing faults. This type of cones is important in studying the interplay between volcanoes and pre-existing basement structures, however further studies are needed to shed light on the tectonic significance of the IVF and its relationships with the East African Rift diffuse plate boundaries (Kusky *et al*., 2010). Moreover, the geomorphological features of multiple and complex cones such as -like shaped and the single cone with multiple craters are the result of complex factors including the existence of fissures/faults and the dynamism of the eruption (Romero, 1991, Dóniz-Páez, 2015). The volcanic cones without craters do exit in the study area; however, they are too small to be mapped by the 30m resolution DEMs, and are covered by pyroclastic material and lava flows from young volcanoes.

Some studies have indicated that the morphometric parameters of volcanic cones could reflect their tectonic settings (e.g. Fornaciai *et al*., 2012, Tibaldi, 1995). Our morphometry analysis reveals that the selected cones are characterized by height-cone base (H_{co}/W_{co}) ratios ranging from 0.07 to 0.24 with an average of 0.15. This average H_{co}/W_{co} ratio (0.15) is slightly lower than those reported for most Quaternary monogenetic volcanic fields (0.17-0.18; e.g. Settle, 1979; Wood, 1980; Dohrenwend *et al*., 1986; Kervyn *et al*., 2012). The maximum H_{co}/W_{co} ratio (0.24) measured within the Itasy volcanic field was obtained from the Ambohitromby cone (with multiple craters), and is more or less similar to those determined for the parasitic cinder cones of the Mt. Etna volcano (e.g. Settle, 1979) and Mauna Kea (Kervyn *et al*., 2012). Fornaciai *et al*. (2012) suggested that cones associated with extensional environment tend to have low average H_{co}/W_{co} ratios (0.11) than those associated with subduction and hot spots (0.15). The average H_{co}/W_{co} value of 0.15 obtained from the selected cones is essentially comparable to those of hot spots; structural and geochemical studies of the IVF are now underway and will provide insights into its petrotectonic origin (Rasoazanamparany *et al.*, in prep; Raharimahefa and Rasoazanamparany, in prep). The compiled data of crater rims will be used to interpret the overall tectonic settings of the IVF and will be published in an accompanying paper (Raharimahefa and Rasoazanamparany, in prep).

Furthermore, we also evaluated the relative ages of the IVF cinder cones on the basis of their morphometric parameters. Some morphometric parameters such as the ratio of cone height to cone base diameter, the maximum cone slope angle, the extent of cone degradation as well as the geomorphological features of lava flows associated with a given cinder cone have been widely used to estimate the relative ages of the cinder cones (Scott and Trask, 1971; Bloomfield, 1975; Wood, 1980b). Most studies indicated that younger cones are often characterized by higher slope angles (e.g. 34° for Paricutin, Mexico) and higher number of gullies (e.g. Hasenaka and Carmichael, 1985), whereas older cinder cones are described to have lower slope angles (e.g. 13° for degraded cones Springerville Volcanic Field, Arizona, Kereszturi and Nemeth, 2012) and have a limited number of larger gullies (Hasenaka and Carmichael, 1985). The semi-circular shaped Kasigie cone is characterized by a conical cone shape with steep slope angles (~40°) and a sharp crater rim. In addition, a larger number of gullies were developed on its flanks, and its crater has little or no sign of significant amount of debris of ash or scoriae from other volcanic eruptions or from the crater itself. Moreover, the cone is associated with well-preserved lava flows with pronounced flow margins and pressure ridges. These characteristics would suggest that the Kasigie volcanic cone represents the youngest cone in the Itasy volcanic field. In contrast, the horseshoe breached cones in the town of Mananasy are characterized by flat and sub-rounded shape with shallow slope angles (Table 1) and show little or no gullies, which would suggest that they are older than the Kasigie cinder cone. However, radiometric Ar-Ar ages of a flow from Kasigie cone yields an eruptive age significantly older than those of Mananasy cinder cones (Rasoazanamparany *et al*., in prep.), implying that the relative ages estimated from the geomorphological parameters of the IVF cones are inconsistent with radiometric ages, and thus caution should be taken when using the geomorphic parameters as ages index.

Our methodological approach enables the characterization of various morphological types of volcanic cones within the Itasy volcanic field, and quantitative morphometric parameters obtained from DEMs have allowed us to describe the size and shape of these volcanic cones. DEMs and Google Earth provided a modern approach in geomorphological study of volcanic cones (Gong *et al*., 2016; Grosse *et al*., 2012). The DEMs are clearly important in a place that topographic maps are not in great details (currently at 1/100,000) and where basic data are lacking. However, field observations are crucial especially when dealing with the slopes and selecting the ground control points.

Conclusion

This contribution has clearly shown that the IVF in central Madagascar contain various volcanic landforms, which are classified into five major types: 1- semi-circular cones, 2- symmetric and asymmetric horseshoes-shaped edifices; 3- fissure cones; 4- multiple clustered breached "ε"-like cones and 5- multiple vents in single large rim. These types of volcanic cones and their morphologies are related to one or a combination of the following factors: the amount of pyroclastic material, the orientation and inclination of the volcanic main vents, dynamic behavior of the vents, previous topography, presence of fissures/ faults, and the dynamism of the eruption.

In this study, morphometric classification of basaltic volcanic cones in the IVF was completed

using field observation, DEMs and satellite images. DEM datasets were extracted from ASTER and SRTM online data and used to characterize the volcanic cones. The use of DEMs coupled with field investigation produced a good morphometric datasets that enable to classified volcanic cones within the IVF. This work has only been able to touch on the most general features of volcanic landforms in the IVF. However, our methodology and approaches are very useful, especially in a place where the scale of topographic maps is not adequate for geomorphometric analyses and mapping of volcanic fields.

In conclusion, we can say that the IVF shared many morphologies and morphometric characteristics with other monogenetic volcanic fields around the world. However, further studies are needed to understand the relationships between each of classified group and the structure of the basement rocks, which will enhance our understanding of the tectonic setting of monogenetic volcanic fields located within stable Precambrian basements.

Acknowledgment

This work was funded by the Faculty of Science, University of Regina research grant to T. Raharimahefa. Thanks to everyone involved in the field works, and we greatly thank the anonymous reviewers and the journal Editor for their keen insight and suggestions.

References

1. Bemis K, Walker J, Borgia A, Turrin B, Neri M, Swisher III C (2011), "The growth and erosion of cinder cones in Guatemala and El Salvador: models and statistics", *Journal of Volcanology and Geothermal Research*, Vol. 20, Nos. 1-4, pp. 39-52.
2. Becerra-Ramirez R (2013), "*Geomorfología y geopatrimonio de los volcanes magmáticos de la Región Volcánica del Campo de Calatrava*", Ph.D. Thesis University of Castilla La Mancha, Spain, p. 818.
3. Bertil D and Regnoult J M (1998), "Seismotectonics of Madagascar", *Tectonophysics*, Vol. 294, pp. 57-74.
4. Bloomfield K (1975), "A late-Quaternary Monogenetic Volcanic Field in Central Mexico", *Geologische Rundschau*, Vol. 64, pp. 476-497.
5. Bussiere P (1957), "*Le Massif Volcanique de l'Itasy Part XII*", in H Besairie, J Boulanger, P Brenon, P Bussiere, A Emberger, J de St. Ours (Eds.), Le Volcanisme à Madagascar, Travaux du Bureau Géologique No. 83, Service Géologique de Madagascar, Tananarive, pp. 1-240.
6. Camiz S, Poscolieri M, Roverato M (2017), "Geomorphometric Comparative Analysis of Latin-America Volcanoes", *Journal of South American Earth Sciences*, Vol. 76, pp. 47-62.
7. Chorowicz J (2005), "The East African Rift System", *Journal of African Earth Sciences*. Vol. 43, pp. 379-410.
8. Connor C B and Conway F M (2000), "Basaltic Volcanic Fields", in H Sigurdsson (Ed.), *Encyclopedia of Volcanoes*, Academic Press, pp. 331-343, New York.
9. Connor C B, Sparks R S J, Díez M, Volentik A C M and Pearson S C P (2009), "The

Nature of Volcanism", in C B Connor, N A Chapman and L J Connor (Eds.), *Volcanic and Tectonic Hazard Assessment for Nuclear Facilities*, pp. 74-115, Cambridge University Press.

10. Corazzato C and Tibaldi A (2006), "Fracture Control on Type, Morphology and Distribution of Parasitic Volcanic Cones: An Example from Mt. Etna, Italy", *Journal of Volcanology and Geothermal Research*, Vol. 158, Nos. 1-2, pp. 177-194.

11. Di Traglia F, Morelli S, Casagli N and Garduño-Monroy V (2014), "Semi-automatic Delimitation of Volcanic Edifice Boundaries: Validation and Application to the Cinder Cones of the Tancitaro–Nueva Italia region (Michoacán–Guanajuato Volcanic Field, Mexico)", *Geomorphology*, Vol. 219, pp.152–160.

12. Dohrenwend J, Wells S, Turrin B (1986), "Degradation of Quaternary cinder cones in the Cima Volcanic Field, Mojave Desert, California", *Geological Society of America Bulletin,* Vol. 97, pp. 421-427.

13. Dóniz-Páez J, Romero C, Coello E, Guillén C, Sánchez N, García-Cacho L, García A (2008), "Morphological and Statistical Characterisation of Recent Mafic Volcanism on Tenerife (Canary Islands, Spain)", *Journal of Volcanology and Geothermal Research,* Vol. 173, Nos. 3-4, pp. 185-195.

14. Dóniz-Páez J, Romero C, Carmona J, García A (2011), "Erosion of cinder cones in Tenerife by Gully Formation, Canary Islands, Spain", *Physical Geography*, Vol. 32, No. 2, pp. 139-160.

15. Dóniz-Páez J, Romero C, Sánchez N (2012), "Quantitative Size Classification of Scoria Cones: The Case of Tenerife (Canary Islands, Spain)". *Physical Geography*, Vol. 33, No. 6, pp. 514-535.

16. Dóniz-Páez J (2015), "Volcanic Geomorphological Classification of the Cider Cones of Tenerife (Canary Islands, Spain)", *Geomorphology*, Vol. 228, pp. 432-447.

17. Favalli M, Fornaciai A (2017), "Visualization and Comparison of DEM-derived Parameters, Application to Volcanic Areas", *Geomorphology*, Vol. 290, pp. 69-84.

18. Fornaciai A, Favalli M, Karátson D, Tarquini S, Boschi E (2012), "Morphometry of Scoria Cones, and Their Relation to Geodynamic Setting: a DEM-based Analysis", *Journal of Volcanology and Geothermal Research*, Vol. 217/218, pp. 56-72.

19. *Gong Li* , Li N, Fan Q, Zhao Y, Zhang L, Zhang C (2016), "*Mapping the topography and cone morphology of the Dalinor* volcanic swarm in Inner Mongolia with remote sensing and DEM data", Frontiers of Earth Science. Vol. 10, pp. 578-594.

20. Grosse P, van Wyk de Vries B, Euillades P A, Kervyn M and Petrinovic I A (2012), "Systematic Morphometric Characterization of Volcanic Edifices Using Digital Elevation Models", *Geomorphology*, Vol. 136, pp. 114-131.

21. Hasenaka T, and Carmichael ISE (1985), "A compilation of location, size, and geomorphological parameters of volcanoes of the Michoacan– Guanajuato volcanic field, central Mexico", Geofisica Internacional. Vol. 24, pp. 577–607.

22. Hickson C, Spurgeon T, Tilling R, Adam P (2013), "Factor Influencing Volcaic Hazards

cnd The Morphology of Volcanic Landforms", in Schorder J F (Ed.), Treatise of *Geomorphology*, Vol 13, pp. 219-242. Academic Press, San Diego.

24. Inbar M, Gilichinsky M, Melekestsev I, Melnikov D and Zaretskaya N (2011), "Morphometric and morphological Development of Holocene Cinder Cones: A Field And Remote Sensing Study In The Tolbachik Volcanic Field, Kamchatka", *Journal of Volcanology and Geothermal Research*, Vol. 201, No. 1-4, pp. 301-331.

25. Kereszturi G and Németh K (2012), "Monogenetic Basaltic Volcanoes: Genetic Classification, Growth, Geomorphology And Degradation", in Németh K (Ed.), *Updates in Volcanology New Advances in Understanding Volcanic Systems*, pp. 3-88 InTech.

26. Kereszturi G, Geyer A, Martí J, Németh K, Dóniz-Páez J (2013a), "Evaluation of Morphometry-based Dating of Monogenetic Volcanoes-a Case Study from Bandas del Sur, Tenerife (Canary Islands)", *Bulletin of Volcanology*, Vol. 75, No. 1, pp. 1-19.

27. Kereszturi G, Németh K, Cronin S, Agustin-Flores J, Smith I, Lindsay J (2013b), "A Model for Calculating Eruptive Volumes for Monogenetic Volcanoes-implication for the Quaternary Auckland Volcanic Field, New Zealand", *Journal of Volcanology and Geothermal Research,* Vol. 266, pp. 16-33.

28. Kervyn M, Ernst G G J, Goossens R and Jacobs P (2008), "Mapping Volcano Topography with Remote Sensing: ASTER vs. SRTM", *International Journal of Remote Sensing*, Vol. 29, No. 22, pp. 6515-6538.

29. Kervyn M, Ernst G G J, Carracedo J-C and Jacobs P (2012), "Geomorphometric Variability of 'Monogenetic' Volcanic Cones: Evidence from Mauna Kea, Lanzarote and Experimental Cones", *Geomorphology*, Vol. 136, pp. 59-75.

30. Kusky T M, Toraman E, Raharimahefa T and Rasoazanamparany C (2010), "Active Tectonics of the Alaotra-Ankay Graben System, Madagascar: Possible Extension of Somalian-African Diffuse Plate Boundary?", *Gondwana Research*, Vol. 18, pp. 274-294.

31. Lenhardt N, Borah S B, Lenhardt S Z, Bumby A J, Ibinoof M A and Salih S A (2018), "The Monogenetic Bayuda Volcanic Field, Sudan – New Insights into Geology and Volcanic Morphology", *Journal of Volcanology and Geothermal Research*, Vol. 356, pp. 211-224.

32. Martin U and Németh K (2006), "How Strombolian is a "Strombolian" Scoria Cone? Some Irregularities in Scoria Cone Architecture from the Transmexican Volcanic Belt, Near Volcán Ceboruco (Mexico), and Al Haruj (Libya)", *Journal of Volcanology and Geothermal Research*, Vol. 155, pp.104-118.

34. Melluso L, le Roex A P and Morra V (2011), "Petrogenesis and Nd-, Pb-, Sr-isotope Geochemistry of the Cenozoic Olivine Melilites and olivine nephelinites ("ankaratrites") in Madagascar", Lithos. Vol. 127, pp. 505-521.

35. Melluso L, Cucciniello C, le Roex A P and Morra V (2016), "The Geochemistry Of Primitive Volcanic Rocks of the Ankaratra Volcanic Complex, And Source Enrichment Processes in the Genesis of the Cenozoic

Magmatism in Madagascar", *Geochimica et Cosmochimica Acta*, Vol. 185, pp. 435-452.

36. Melluso L, Tucker RD, Cucciniello C, le Roex AP, Morra V, Zanetti A, Rakotoson RL (2018), "The Magmatic Evolution and Genesis of the Quaternary Basanite-Trachyphonolite Suite of Itasy (Madagascar) as Inferred by Geochemistry, Sr-Nd-Pb Isotopes and Trace Element Distribution in Coexisting Phases", *Lithos*, Vol. 310-311, pp. 50-64.

37. Németh K (2010), "Monogenetic Volcanic Fields: Origin, Sedimentary Record, and Relationship With Polygenetic Volcanism" in E Cañón-Tapia and A. Szakács (Eds.), *What Is a Volcano?, Geological Society of America Special Paper,* Vol. 470, pp. 43-66.

38. Petit C, Déverchère J (2016), "Structure and Evolution of the Baikal rift: a Synthesis", *Geochemistry, Geophysics, Geosystems*, Vol. 7. No. 11, pp. 1-26.

39. Prima O D A and Yoshida T (2010), "Characterization of Volcanic Geomorphology and Geology by Slope and Topographic Openness", *Geomorphology*, Vol. 118, pp. 22-32.

40. Putirka K, Platt B (2012), "Basin and Range Volcanism as a Passive Response to Extensional Tectonics", *Geosphere*, Vol. 8, No 6, pp. 1274-1285.

41. Rakotondraompiana (1992), "*Gravimetrie de Madagascar et structure de la lithosphere"*, These Universite d'Antana-narivo.

42. Rakotondraompiana S A, Albouy Y and Pique A (1999), "Lithospheric Model of the Madagascar Island (western Indian Ocean): a New Interpretation of the Gravity Data", *Journal of African Earth Sciences*, Vol. 28, pp. 961-973.

43. Razafiniparany A, Joo J, Rakotomavo G , Rakotoarivony X (1974), "Carte Géologique Soavinandriana (M47) (1/100,000)", *Service Géologique, Antananarivo, Madagascar*.

44. Rechenmann J (1981), "*Gravimetrie de Madagascar, interpretation et relations avec la geologie", Editions de l'office a la recherché*, ORSTROM, France.

45. Rindraharisaona E J, Guidarelli M, Aoudia A and Rambolamanana G (2013), "Earth Structure and Instrumental Seismicity of Madagascar: Implications on the Seismotectonics", *Tectonophysics*, Vol. 594, pp. 165-181.

46. Riedel C, Ernst G G J and Riley M (2003), "Controls on the Growth and Geometry of Pyroclastic Constructs", *Journal of Volcanology and Geothermal Research*, Vol. 127, Nos. 1-2, pp. 121-152.

47. Rittmann A (1963), "*Les Volcans et Leur Sctibite*", Masson, p. 461, Paris.

48. Rodríguez E, Morris C S and Belz J E (2006), "A Global Assessment of the SRTM Performance", *Photogrammetric Engineering and Remote Sensing*, Vol. 72, pp. 249-260.

49. Rodríguez S R, Morales-Barrera W, Layer P, González-Mercado E (2010), "A Quaternary Monogenetic Volcanic Field in the Xalapa Region, Eastern Trans-Mexican Volcanic Belt: Geology, Distribution and Morphology of the Volcanic Vents", *Journal of Volcanology and Geothermal Research*, Vol. 197, Nos. 1-4, pp. 149-166.

50. Romero C (1991), "Las Manifestaciones Volcánicas Históricas del Archipiélago

Canario", *Consejería de Política Territorial Gobierno Autónomo de Canarias*, Santa Cruz de Tenerife", p. 1463.

51. Rufer D, Preusser F, Schreurs G, Gnos E, Berger A (2014), "Late Quaternary History of the Vakinankaratra volcanic field (central Madagascar): Insights From Luminescence Dating of Phreatomagmatic Eruption Deposits", *Bulletin of Volcanology*, Vol. 76, No. 817, pp. 1-20.

52. Scott DH and Trask NJ (1971), "Geology of the Lunar Crater volcanic field, Nye County, Nevada", *US Geological Survey Professional Paper 599-I*.

53. Settle M (1979), "The Structure and Emplacement of Cinder Cone Fields". American Journal of Science 279, pp. 1089-1107.

54. Takada A (1994), "The Influence of Regional Stress And Magmatic Input on Styles of Monogenetic and Polygenetic Volcanism", J*ournal of Geophysical Research,* Vol. 99, No. B7, pp. 13563–13573.

55. Tibaldi A (1995), "Morphology of Pyroclastic Cones and Tectonics". *Journal of Geophysical Research,* Vol. 100, No. B12, pp. 24521–24535.

56. Tibaldi A, Lagmay A (2006), "Interaction Between Volcanoes And Their Basements", *Journal of Volcanology and Geothermal Research*, Vol. 158, pp. 1-5.

57. Thouret J C (1999), "Volcanic Geomorphology - An Overview", *Earth Sciences Reviews*, Vol. 47, pp. 95-131.

58. Tucker R D, Roig Y G, Moine B, Delor C and Peters S G (2014), "A Geological Synthesis of the Precambrian Shield in Madagascar", *Journal of African Earth Sciences*, Vol. 94, pp. 9-30.

59. Valentine GA, Perry FV, Krier D, Keating GN, Kelley RE, Cogbill AH (2006), "Small-volume Basaltic Volcanoes: Eruptive Products and Processes, and Posteruptive Geomorphic Evolution in Crater Flat (Pleistocene), Southern Nevada", *Geological Society of America Bulletin*, Vol. 118, Nos. 11-12, pp. 1313-1330.

60. Valentine G, Krier D, Perry F, Heinken G (2007), "Eruptive and Geomorphic Processes at the Lathrop Wells scoria cone Volcano", *Journal of Volcanology and Geothermal Research*, Vol. 161, pp. 57-80.

61. Valentine G A and Gregg T K P (2008), "Continental Basaltic Volcanoes—Processes and Problems", *Journal of Volcanology and Geothermal Research*, Vol. 177, No. 4, pp. 857-873

62. Vogel (1970), "Groningen Radio-carbon Dates IX", *Radiocarbon,* Vol. 12, pp. 444-471.

63. Wood C A (1980a), "Morphometric Evolution of Cinder Cones", *Journal of Volcanology and Geothermal Research*, Vol. 7, pp. 387-413.

64. Wood C A (1980b), "Morphometric Analysis of Cinder Cone Degradation", *Journal of Volcanology and Geothermal Research*, Vol. 8, pp. 137-160.